Int. J. Electrochem. Sci., 14 **(2019)** 1416 – 1422, doi: 10.20964/2019.02.69

International Journal of
ELECTROCHEMICAL
SCIENCE
www.electrochemsci.org

Hollow Fe_3O_4 Spheres as Efficient Sulfur Host for Advanced Electrochemical Energy Storage

Yanhua Wang[1], *Jianying Tong*[1], *Kefeng Xie*[2,*]

[1] College of Biology and Environmental Engineering, Zhejiang Shuren University, Hangzhou 310000, China
[2] State Key Laboratory of Plateau Ecology and Agriculture, Qinghai University, Xining 810016, China
[*]E-mail: xiekefeng@qhu.edu.cn

Received: 19 October 2018 / *Accepted:* 4 December 2018 / *Published:* 5 January 2019

Among various electrochemical energy storage systems, Li-S batteries are one of the most promising candidates. However, the application of Li-S batteries is mainly hindered by the shuttle effect of soluble polysulfide. To inhibit this shuttle effect, hollow Fe_3O_4 spheres (HFS) are prepared and used as host materials for sublimed sulfur. Due to the strong absorption between Fe_3O_4 spheres and polysulfide, the as-prepared S@HFS composites exhibit excellent cycle stability. As a result, the S@HFS composites show a high initial specific capacity of 1310 mAh g^{-1} at 0.1 C.

Keywords: S@HFS; cathode material, host, absorption, electrochemical performance

1. INTRODUCTION

Lithium-sulfur batteries are the most promising candidates for the next energy storage system. In the past decades, many efforts have been made to develop advanced Li-S batteries [1, 2, 3]. To achieve the excellent electrochemical performance, various cathode materials have been prepared. After that, modified separators become a hot topic for the scientists in the Li-S area [4, 5]. More recently, electrolytes for the battery are greatly studied for improving the electrochemical performances [6, 7]. With the deep understanding for Li-S battery, researchers find that it have to design optimal host materials for sulfur to improve the electrochemical performance [8, 9, 10]. As a result, many teams put their eyes from the separators and electrolyte to the cathode materials again.

Due to the shuttle effect of polysulfide, which is produced during discharging process, the cathode materials should have a character of immobilizing the polysulfide on the cathode side [11, 12]. To satisfy this demand, various host materials are reported in the literatures, including carbon materials [13], metal oxides [14], metal sulfides [15], metal hydroxides [16] and other transition metal composites.

In this work, hollow Fe_3O_4 spheres were successfully synthesized and employed as efficient host for advanced electrochemical energy storage. On the one hand, the hollow Fe_3O_4 spheres provide sufficient active site for polysulfide absorption. On the other hand, the use of hollow Fe_3O_4 spheres could enhance the electronic conductivity off the whole cathode material. Therefore, the as-prepared S@HFS electrodes exhibit high specific capacity and excellent cycle stability.

2. EXPERIEMENTAL

2.1. Preparation of S@HFS composite

Polystyrene, $FeCl_3 \cdot 6H_2O$, $FeCl_2 \cdot 4H_2O$ and polyvinyl pyrrolidone were purchased from Shanghai Huayi Group. Ammonia, ethanol and sublimed sulfur were purchased from Aladdin. All reagents used were of analytical grade without further purification. First, 2.12g polystyrene (PS) spheres, 6.15g $FeCl_3 \cdot 6H_2O$ and 3.02g $FeCl_2 \cdot 4H_2O$ were dissolved into 100ml ethanol. 2.15ml ammonia and 1.13g polyvinyl pyrrolidone (PVP) were added into the above solution under magnetic stirring. Then, the mixed solution was transferred into vacuum oven at 120℃ for 3h. After that, the products were washed and dried. The obtained sample was then heated at 500℃ for 5h to remove the polystyrene. As a result, the hollow Fe_3O_4 spheres were obtained. For the preparation of S@HFS composite, the HFS and sublimed sulfur were mixed with a ratio of 1:1, and then were heated at 155℃ for 10 h under Ar atmosphere. Finally, the S@HFS composite was obtained.

2.2. Materials Characterization

The morphology of as-prepared S@HFS composite was characterized by transmission electron microscope (JEM-2010HR). The content of sulfur in the S@HFS composite was obtained via thermogravimetric analysis (TA Q600).

2.3. Electrochemical Performance

The electrochemical performance of S@HFS composite was tested by assembling CR2032 coin batteries. The separator type is Celgard2300. The S@HFS composite electrode and lithium electrode were cathode and anode, respectively. The electrolyte is consisted of 1 M LITFSI, DOL/DME (1:1), 2% $LiNO_3$. The discharge/charge profiles are obtained from LAND tester between 1.5 V and 3.0 V. Cyclic voltammetry curves are tested on the electrochemical workstation (CHI660E) between 1.5 V and 3.0 V with a scanning rate of 0.1 mV s^{-1}.

3. RESULTS AND DISCUSSION

The preparation process of hollow Fe_3O_4 spheres is illustrated in Figure 1. As shown in Figure 1, polystyrene (PS) spheres, $FeCl_3 \cdot 6H_2O$ and $FeCl_2 \cdot 4H_2O$ were firstly dissolved into ethanol. Then,

ammonia and PVP were added into the above solution. Next, the mixed solution was transferred into vacuum oven at 120℃ for 3h. After that, the obtained sample was then heated at 500℃ for 5h to remove the polystyrene. As a result, the hollow Fe_3O_4 spheres were obtained. Next, the S@HFS composites were obtained by heating the HFS and sublimed sulfur at 155 ℃ for 10 h. Finally, the S@HFS composites were prepared successfully.

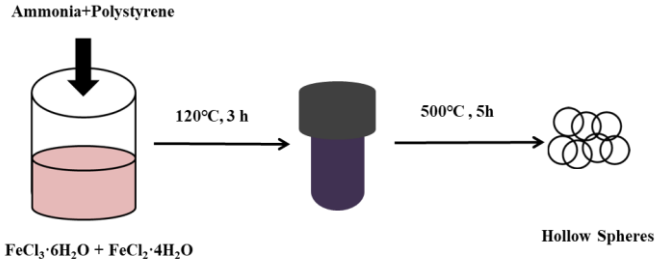

Figure 1. The preparation of hollow Fe_3O_4 spheres.

To observe the morphologies of the samples, transmission electron microscope test was conducted. As shown in Figure 2a, the as-prepared Fe_3O_4 materials display hollow sphere structure. And the hollow Fe_3O_4 spheres are uniformly distributed. The dimeter of HFS ranges from 50 nm to 80 nm. After heating with sublimed sulfur, the S@HFS composites are obtained. Figure 2b shows the TEM image of S@HFS composites. It can be seen that black particles are located in the hollow sphere structure. This indicates the presence of sulfur in the S@HFS composites. Figure 2c exhibits the TEM image of S@HFS composites at high magnification. To further demonstrate the element distribution in the S@HFS composites, EDS was tested for the S@HFS composites. From Figure 2e-g, it can be clearly observed that the elements Fe, O, S are uniformly distributed in the S@HFS composites.

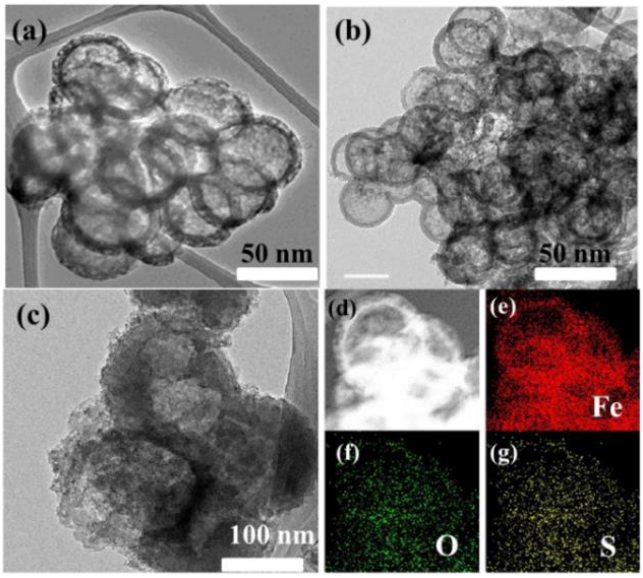

Figure 2. TEM images of (a) HFS, (b) S@HFS, (c) and (d)TEM images of S@HFS at high magnification, Elemental mapping of (e) Fe, (f) O, (g) S.

The content of sulfur in the S@HFS composites is determined by TG analysis. This is because the specific capacity value is calculated according to the sulfur mass in the S@HFS composites. As shown in Figure 3, it can be calculated that the sulfur content is 49.86% in the S@HFS composites. Therefore, the sulfur loading on the electrode could be obtained. Finally, the specific capacity value could be calculated by the sulfur loading on the electrode [17].

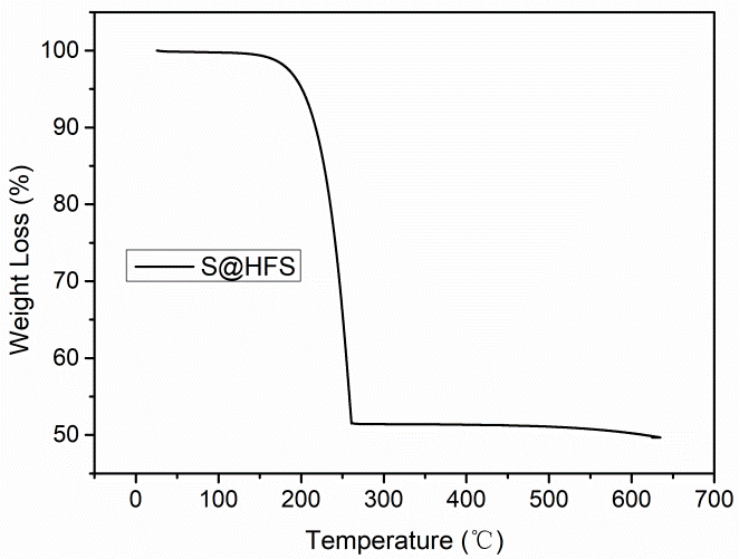

Figure 3. TG curve of S@HFS composite.

To verify the electrochemical performance of the S@HFS composites, various electrochemical tests are conducted. Figure 4a is the initial DC profiles of two samples electrodes at the current density of 0.1 C. The S@HFS composites display a high specific discharge capacity value of 1310 mAh g^{-1}, while the specific discharge capacity value of sublimed sulfur electrode is 1103 mAh g^{-1}. Obviously, the S@HFS composites show higher capacity value than the sublimed sulfur electrode. This improved specific capacity value is mainly due to the presence of HFS, which could enhance the electronic conductivity of the whole electrode [18]. As a result, the S@HFS composite electrode exhibits higher capacity value than pure the sulfur electrode.

The capacity value at various current densities is a key factor for the Li-S batteries. Therefore, the discharge capacity value of S@HFS composites are tested at 0.1 C, 0.2 C, 0.5 C, 1 C, 2 C, respectively. As shown in Figure 4b, with the increase of current density, the capacity value decreases rapidly. This phenomenon is caused due to the electrochemical polarization at high current densities. Especially, it can be clearly observed from the Figure when the current density was improved form 0.2 C to 0.5 C, the capacity fades rapidly.

Cyclic voltammetry is a perfect method to investigate the redox reaction mechanism in the Li-S battery system. As shown in Figure 4c, the CV curve of S@HFS composite was tested at a scan rate of 0.1 mV s^{-1} from 1.5 V to 3.0 V. Two cathodic peaks are clearly observed at 2.0 V and 2.3 V, respectively. These two peaks are corresponding to the two voltage platform in the discharge profile. It represents two step reduction of sulfur particle: from sulfur to soluble polysulfide, soluble polysulfide to Li_2S, respectively. All in all, two step reduction and one step oxidation are observed in the Li-S battery system. This is consistent with previous reports [19].

Rate performance is another important index for measuring the performance of Li-S battery. As shown in Figure 4d, the S@HFS composite could tolerate various current densities. Even when the current density is improved to 2 C, the specific capacity of S@HFS could remain at 806 mAh g^{-1}. Moreover, when the current density returns 0.1 C, the specific capacity could recover back its initial capacity value. Rate performance represents the ability of the electrode at high current densities. From the Figure 4d, it can be seen that the S@HFS composite electrode could still provide high capacity value at the current density of 2 C. This electrochemical performance is more excellent than other reports [20, 21]

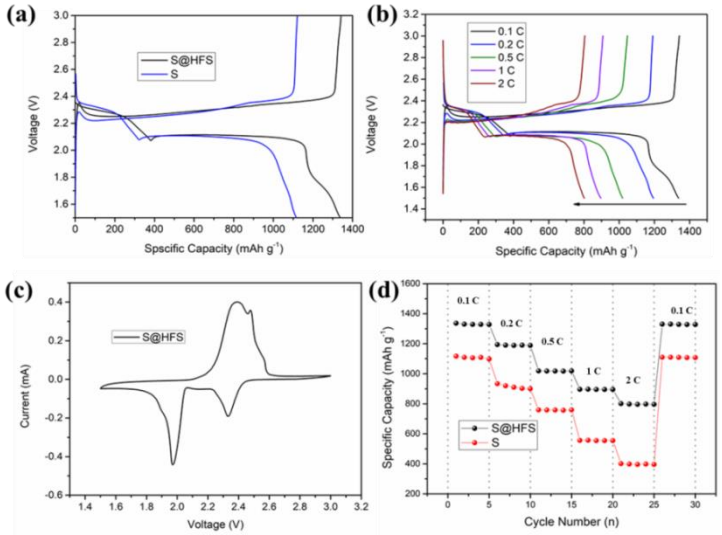

Figure 4. (a) The first DC profiles of two samples electrodes at 0.1 C. (b) The DC profiles of S@HFS electrode at kinds of current densities. (c) The CV curves of S@HFS electrode at 0.1 mV s^{-1}. (d) Rate performance of two samples electrodes.

Figure 5a demonstrates the cycle performance of S@HFS electrode at 1 C after 300 cycles. An energy storage system must provide energy for a long period time cycle. This is an important factor for its application in the future. As shown in Figure 4a, the capacity value of S@HFS composite remains 783 mAh g^{-1} after 300 cycles, indicating an excellent electrochemical performance. According to the EIS (Figure 5b), it can be concluded that the impedance of S@HFS composite is much smaller than the sublimed sulfur. Clearly, it can be observed the ability of charge transferring for the S@HFS composite is stronger than pure sulfur electrode. This result is consistent with the higher specific capacity value in Figure 4a.

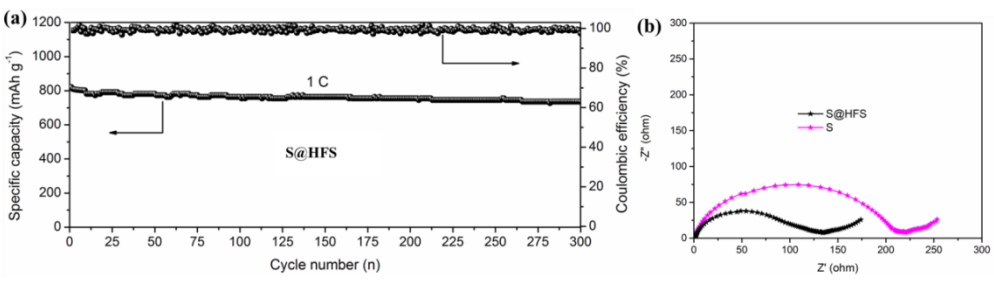

Figure 5. (a) Cycle performance of S@HF electrode after 300 cycles. (b) EIS of two samples electrodes.

Table 1 lists the electrochemical performances of various cathode materials in Li-S batteries. It can be seen that from the table, the as-prepared S@HFS composite electrode shows excellent cycle stability. The S@HFS electrode shows capacity value of 783 mAh g^{-1} after 300 cycles at 1 C. However, the capacities other similar cathode materials fade rapidly. This result further confirms the superior electrochemical performance.

Table1. Electrochemical performances of various cathode materials in the Li-S batteries

Samples	Rates (C)	Specific Capacity (mAh g^{-1})	References
S@HFS	1	783 (300)	This Work
MCMB/S	1	246 (100)	22
S/NC	0.5	760 (100)	23
PANI@S-OMC/S	0.5	671 (500)	24
Mo_2N/S	0.5	771 (200)	25

4. CONCLUSIONS

In summary, we have successfully prepared hollow Fe_3O_4 spheres. The HFS shows uniformly hollow sphere structure. Then, the HFS is applied as sulfur cathode materials. The electrochemical results indicate that the as-prepared S@HFS composites display excellent cycle stability and superior rate performance. All of these perfect electrochemical performances are attributed to the hollow sphere structure of Fe_3O_4, which could provide enough absorption for the soluble polysulfide. Besides, the EIS result demonstrates smaller impedance of S@HFS composite than sublimed sulfur. As a result, the S@HFS composite shows capacity value of 783 mAh g^{-1} after 300 cycles.

ACKNOWLEDGMENTS
We thank Qinghai University for technical support.

References

1. M. K. Nagao, K. Suzuki, Y. K. Imade, M. Tateishi and R. J. Kanno, *J. Power Sources*, 330 (2016) 120.
2. S. K. Lee, Y. J. Lee and Y. K. Sun, *J. Power Sources,* 323 (2016) 174.
3. Z. L. Peng, R. G. Li, J. D. Gao, Z. X. Yang, Z. H. Deng and J. S. Suo, *Electrochim. Acta*, 220 (2016) 130.
4. R. Xu, Y. Z. Sun, Y. F. Wang, J. Q. Huang, Q. Zhang, *Chinese Chem. Lett*., 28 (2017) 2235.
5. Y. Li, J. Chen, Y. F. Zhang, Z. Y. Yu, T. Z. Zhang, W. Q. Ge and L. P. Zhang, *J. Alloy Compd*., 766

(2018) 804.
6. H. Huang, J. G. Yu, Y. P. Gan and Y. Xia, *Mater. Res. Bull*., 96 (2017) 425.
7. Q. Cheng, C. Liu, K. Meng, X. H. Yu, Y. N. Zhang, J. X. Liu, X. Jin and L. Y. Jin, *Int. J. Electrochem. Sci*., 13 (2018) 265.
8. L. T. Yan, J. L. Yu and H. M. Luo, *Appl. Mater. Today,* 8 (2017) 31.
9. X. J. Liu, N. Xu, T. Qian, J. Liu, X. W. Shen and C. L. Yan, *Nano Energ*., 41 (2017) 758.
10. N. J. Song and C. L. Ma, *Int. J. Electrochem. Sci.*, 13 (2018) 452.
11. O. K. Park, Y. H. Cho, S. H. Lee, H. C. Yoo, H. K. Song and J. Cho, *Energ. Environ. Sci*., 4 (2011) 1621.
12. J. H. Xu, B. Jin, H. Li and Q. Jian, *Int. J. Hydrogen. Energ*., 42 (2017) 20749.
13. J. Rao, R. T. Xu, T. F. Zhou, D. W. Zhang and C. F. Zhang, *J. Alloy Compd*., 728 (2017) 376.
14. Y. L. Deng, J. Y. Li, T. H. Li, X. F. Gao and C. Yuan, *J. Power Sources*, 343 (2017) 284.
15. L. Zhang, M. Ling, J. Feng, G. Liu and J. H. Guo, *Nano Energ*y, 40 (2017) 559.
16. L. L. Zhang, Y. J. Wang, Z. Q. Niu and J. Chen, *Carbon*, 141 (2019) 400.
17. R. L. Yang, H. W. Du, Z. Q. Lin, L. L. Yang, H. Zhu, H. Zhang, Z. K. Tang and X. C. Gui, *Carbon*, 141 (2019) 258.
18. P. Zhang, W. B. Yue and R. L. Li, *Electrochim. Acta*, 282 (2018) 595.
19. H. Tan, K. Huang, Y. X. Bao, Y. Li and J. X. Zhong, *J. Alloy Compd*., 699 (2017) 812.
20. S. X. Jiang, M. F. Chen, X. Y. Wang, Y. Zhang, C. Huang, Y. P. Zhang and Y. Wang, *Chem. Eng. J*., 355 (2019) 478.
21. Y. Song, H. Wang, W. S. Yu, J. X. Wang, G. X. Liu, D. Li, T. T. Wang, Y. Yang, X. T. Dong and Q. L. Ma, *J. Power Sources*,405 (2018) 51.
22. W. T. Tsou, C. Y. Wu, H. Yang and J. G. Duh, *Electrochim. Acta*, 285 (2018) 16.
23. N. Li, X. He, K. H. Chen, S. Y. Chen and F. Y. Gan, *Mater. Lett*., 228 (2018) 195.
24. Z. W. Ding, D. L. Zhao, R. R. Yao, C. Li, X. W. Cheng and T. Hu, *Int. J. Hydrogen Energ*y, 43 (2018) 10502.
25. G. S. Jiang, F. Xu, S. H. Yang, J. P. Wu, B. Q. Wei and H. Q. Wang, *J. Power Sources*, 395 (2018) 77.